DOI: 10.1002/rem.21593

RESEARCH ARTICLE

WILEY

Evaluating the longevity of a PFAS *in situ* colloidal activated carbon remedy

Grant R. Carey[1] | **Rick McGregor**[2] | **Anh Le-Tuan Pham**[3] | **Brent Sleep**[4] | **Seyfollah Gilak Hakimabadi**[3]

[1]Porewater Solutions, Ottawa, Ontario, Canada

[2]In Situ Remediation Services Ltd., St. George, Ontario, Canada

[3]University of Waterloo, Waterloo, Ontario, Canada

[4]University of Toronto, Toronto, Ontario, Canada

Correspondence
Grant R. Carey, Porewater Solutions, 27 Kingsford Cresent, Ottawa, Ontario K2K 1T5, Canada.
Email: gcarey@porewater.com

Abstract

The remediation of per- and polyfluoroalkyl substances by injection of colloidal activated carbon (CAC) at a contaminated site in Central Canada was evaluated using various visualization and modeling methods. Radial diagrams were used to illustrate spatial and temporal trends in perfluoroalkyl acid (PFAA) concentrations, as well as various redox indicators. To assess the CAC adsorption capacity for perfluorooctane sulfonate (PFOS), laboratory Freundlich isotherms were derived for PFOS mixed with CAC in two solutions: (1) PFOS in a pH 7.5 synthetic water that was buffered by 1 millimolar $NaHCO_3$ (K_f = 142,800 mg^{1-a} L^a/kg and a = 0.59); and (2) a groundwater sample (pH = 7.4) containing PFOS among other PFAS from a former fire-training area in the United States (K_f = 4,900 mg^{1-a} L^a/kg and a = 0.24). A mass balance approach was derived to facilitate the numerical modeling of mass redistribution after CAC injection, when mass transitions from a two-phase system (aqueous and sorbed to organic matter) to a three-phase system that also includes mass sorbed to CAC. An equilibrium mixing model of mass accumulation over time was developed using a finite-difference solution and was verified by intermodel comparison for prediction of CAC longevity in the center of a source area. A three-dimensional reactive transport model (ISR-MT3DMS) was used to indicate that the CAC remedy implemented at the site is likely to be effective for PFOS remediation for decades. Model results are used to recommend remedial design and monitoring alternatives that account for the uncertainty in long-term performance predictions.

1 | INTRODUCTION

Per- and polyfluoroalkyl substances (PFAS) are emerging contaminants that are widespread in the environment and are generally persistent (Hatton, Holton, & DiGuiseppi, 2018). Perfluoroalkyl acids (PFAAs) are the main types of PFAS that are analyzed in soil and groundwater at contaminated sites and generally have low regulatory advisory or cleanup levels. Some PFAS precursors are known to undergo aerobic biodegradation (e.g., Avendano & Liu, 2016; Harding-Marjanovic et al., 2015), where transformation products may include PFAAs. PFAAs have not been observed to undergo biological or abiotic transformation reactions, resulting in persistent plumes at many sites (Hatton et al., 2018).

There are two classes of PFAAs: perfluoroalkyl carboxylates (PFCAs) and perfluoroalkyl sulfonates (PFSAs). The most commonly regulated PFAS in the environment are perfluorooctanoate (PFOA), which is a PFCA, and perfluorooctane sulfonate (PFOS), which is a PFSA. Regulatory cleanup criteria for these and other PFAS are undergoing development; at present, the U.S. Environmental Protection Agency (USEPA) has imposed a Lifetime Health Advisory for PFOS and PFOA individually or in combination, of 0.07 microgram per liter (μg/L; USEPA, 2016a, 2016b). Health Canada drinking water screening values for PFOS and PFOA are 0.6 and 0.2 μg/L, respectively (Health Canada, 2018). These low cleanup levels and the persistent nature of PFAAs pose a significant challenge in remediating PFAS sites.

Granular activated carbon (GAC) is effective for *ex situ* treatment of PFAS in groundwater in some cases (McCleaf et al., 2017). GAC has a typical particle size range of 500 to 1,000 μm, and powdered activated carbon (PAC) may have a particle size of 10 to 100 μm. USEPA (2018) presents a summary of the practice of injecting activated carbon *in situ* as a remediation approach for chlorinated solvents and petroleum hydrocarbons. This includes the high-pressure injection of GAC or PAC, which induces fracturing leading to the heterogeneous distribution of GAC and PAC in thin seams or lenses (USEPA, 2018). Another alternative now being employed is the low-pressure injection of colloidal

activated carbon (CAC) with particle sizes of 1 to 2 μm, which does not induce fracturing and results in a more uniform distribution of activated carbon in the target treatment zone (USEPA, 2018). CAC can be readily injected into fine to coarse sand aquifers (grain sizes of 60–70 μm and greater).

In the case of PFAAs, *in situ* CAC injection may be conducted in a grid pattern to reduce the mass flux from a source zone, or CAC may be injected in a permeable barrier to intercept a plume. Previous work with PFAS sorption to GAC indicates that activated carbon has a high sorption capacity for some PFAS (Appleman et al., 2014; McCleaf et al., 2017). Yu, Zhang, Deng, Huang, and Yu (2009) determined that the sorption capacity associated with activated carbon is higher for smaller sized particles of activated carbon (e.g., PAC versus GAC), because the smaller particles have a higher external surface area per mass of activated carbon. PFAS will eventually break through when the adsorption capacity of *in situ* CAC becomes depleted (USEPA, 2018). Models incorporating Freundlich adsorption behavior and a mechanism for redistributing PFAS mass after CAC injection can be used to assess the longevity of a CAC remedy, and the frequency at which additional CAC may need to be injected to prevent breakthrough.

The benefits of a radial diagram visualization method for assessing the distribution of numerous PFSAs and PFCAs in monitoring wells are demonstrated.

McGregor (2018) presented a case study in which PFOS and PFOA were successfully immobilized through *in situ* injection of CAC at a site in Central Canada. The current study develops a numerical model to evaluate the longevity of this *in situ* remediation approach for this site. The benefits of a radial diagram visualization method for assessing the distribution of numerous PFSAs and PFCAs in monitoring wells are demonstrated. PFOS-CAC isotherms are presented based on laboratory experiments involving a pH 7.5 synthetic solution containing only PFOS and 1 millimolar (mM) $NaHCO_3$ (which serves as a pH buffer; 1 mM HCO_3^- is also a typical alkalinity of groundwater), and a PFAS mixture in a groundwater sample (pH 7.4) collected at a former fire-training area in the United States. A mass balance is incorporated into a numerical model to simulate the redistribution of mass from the original two-phase system (aqueous and sorbed to soil organic matter), to the three-phase system after CAC injection (including sorption to CAC attached to sand grains). An equilibrium mixing model (EMM) is developed for estimating CAC longevity in the middle of a source zone. A sensitivity analysis is conducted to evaluate the range in longevity from a single CAC injection based on isotherm parameters and the fraction of CAC retained in the injection zone.

2 | STUDY SITE

The implementation of the *in situ* CAC remedy at the study site in Central Canada is summarized by McGregor (2018). Occasional fire-training activities at the site resulted in a low-level PFAS plume at the site, with preremedy concentrations of PFOS and PFOA up to approximately 1.5 and 3.3 μg/L, respectively. There were also localized sources of petroleum hydrocarbons in different portions of the site due to other activities. The shallow overburden aquifer at the site is composed of medium sand with some silt. The vertical interval impacted by PFAS at the site occurred over a depth of 0.9 to 1.7 meters (m) below ground surface. The average hydraulic conductivity was 2.6 meters per day (m/d), and the average horizontal hydraulic gradient was 0.06 m/m. Based on an effective porosity of 0.2 m^3/m^3, the average linear groundwater velocity was 0.8 m/d.

The *in situ* remediation approach involved the low-pressure injection of CAC and an oxygen-releasing material into the shallow overburden aquifer. Fifty temporary injection wells were used in total at the site with a grid spacing of approximately 3 m, although only about half of those wells were needed in the vicinity of the PFAS source. Proprietary additives including an organic polymer are included in the CAC solution to stabilize CAC and to facilitate transport in the subsurface. The injection event was conducted over a two-day period in spring 2016 at a cost of less than CAD$100,000.

McGregor (2018) indicates that CAC was observed at a distance up to 4.6 m from an injection point based on soil samples collected at multiple locations and depth intervals 19 months after the injection event. The average fraction of CAC (f_{cac}) measured in the target zone after injection was approximately 0.02% (i.e., 0.23 grams per kilogram) with a maximum measured concentration of 0.04%. The fraction of organic carbon (f_{oc}) was measured to be 0.001% outside the target treatment zone.

Exhibit 1 shows the location of the suspected PFAS source area, the extent of the CAC zone postinjection in the vicinity of this PFAS source zone, and charts of PFOS concentration versus time at monitoring wells with available data (MW-1, MW-2, MW-5, and MW-8). The PFAS source area has an average length of 6.5 m, width of 4.5 m, and an area of 30 m^2. The CAC zone shown in Exhibit 1 extends 10 m downgradient of the PFAS source area. This creates a CAC buffer downgradient of the source area, which helps to increase the remedy longevity, as discussed further below. The extent of the CAC zone was approximated by delineating an area that extended approximately 3 m outside the grid of temporary injection wells. (The northern extent of the CAC zone that was used to remediate only petroleum hydrocarbons is not shown in Exhibit 1.)

The charts shown in Exhibit 1 illustrate that the concentration of PFOS in groundwater was reduced by orders of magnitude (below the detection limit of 0.03 μg/L) after the CAC injection. There was only one detection of PFOS at 0.04 μg/L approximately 1.5 years after the CAC injection event, although PFOS was not detected in a subsequent monitoring round conducted approximately 2 years after the injection event. The source of PFOS detected at one well in this single monitoring event is uncertain and may be due to cross-contamination in the field or in the laboratory.

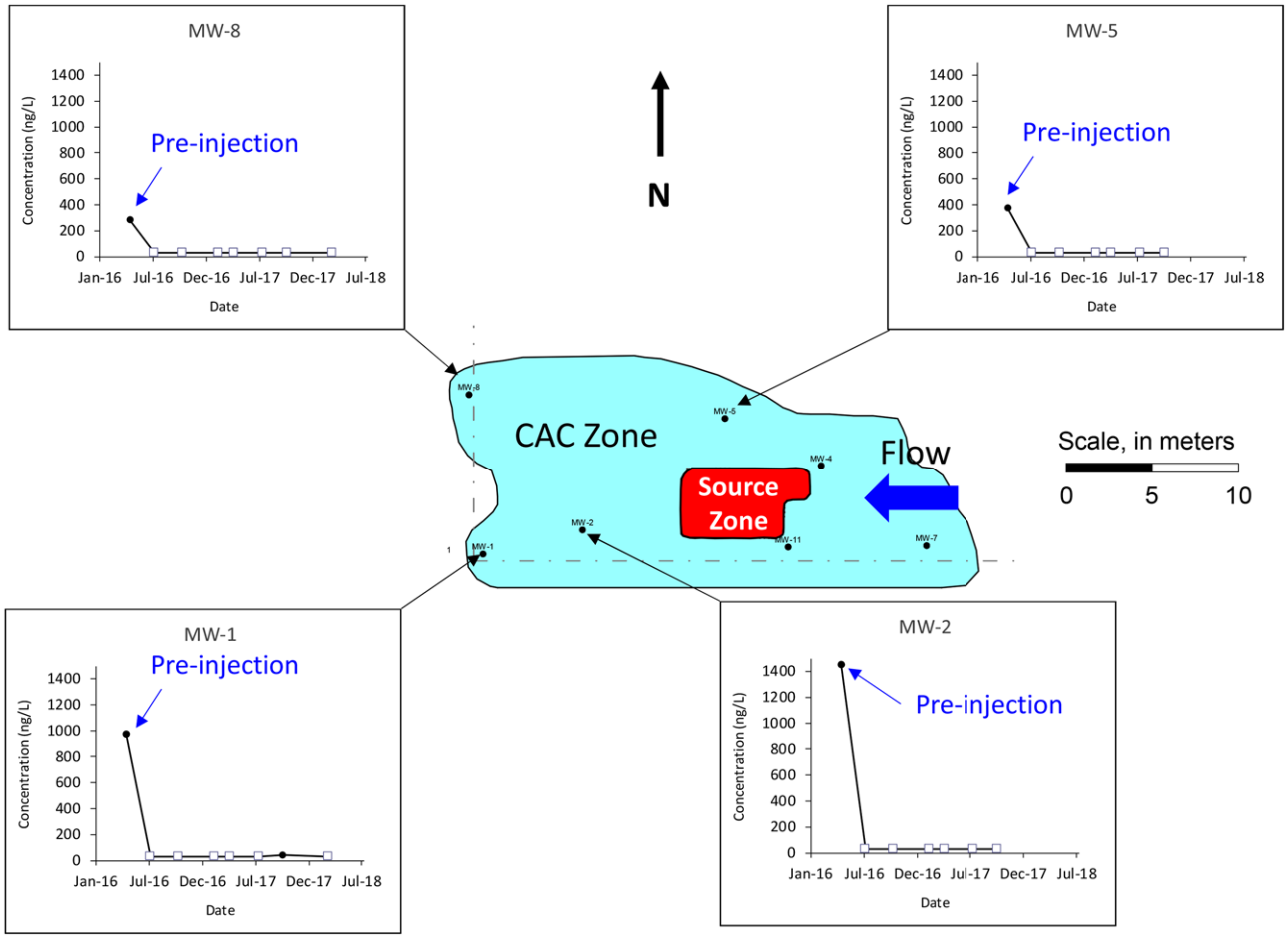

EXHIBIT 1 PFOS concentrations versus time charts (Note that the CAC injection event was in spring 2016)

2.1 | Radial diagram visualization

Carey et al. (1999, 2003) discussed how radial diagrams may be effective for evaluating both spatial and temporal trends for petroleum hydrocarbons, chlorinated solvents, and/or reduction-oxidation (redox) indicators. Given the multispecies nature of PFAS mixtures at many sites, radial diagrams may also be effective for visualizing trends for PFAS at contaminated sites.

During initial monitoring events at the site, only PFOS and PFOA were analyzed. In October 2017, a suite of PFAAs were analyzed to see if other PFAS constituents were detectable in groundwater after the CAC injection event. Exhibit 2 presents radial diagrams representing nine PFCAs that were analyzed in October 2017, including perfluorobutanoate (PFBA), perfluoropentanoate (PFPeA), perfluorohexanoate (PFHxA), perfluoroheptanoate (PFHpA), PFOA, perfluorononanoate (PFNA), perfluorodecanoate (PFDA), perfluoroundecanoate (PFUnA), and perfluorododecanoate (PFDoA). The legend shown at the top right of Exhibit 2 represents PFCA concentrations at a single monitoring well (MW-1), where each axis of the radial diagram represents the concentration of a single PFCA constituent. The axes of the radial diagram are ordered counterclockwise in the sequence of increasing molecular chain length. The orange-shaded data series represents October 2017 concentrations for each PFCA. A white symbol is used to represent nondetects and is plotted at a concentration equivalent to one-half of the detection limit. A single black symbol is used to show the preinjection PFOA concentration injection (when the other constituents were not analyzed).

Radial diagrams are shown for five monitoring wells at the site in Exhibit 2; four wells within the CAC zone (MW-1, MW-2, MW-5, and MW-8), and one well outside the CAC zone (MW-9) where PFOA was not detected prior to CAC injection. Comparison of the preinjection and October 2017 PFOA concentrations at monitoring wells within the CAC zone indicates that PFOA concentrations were still reduced by at least one order of magnitude 19 months after the injection event. There was only one detection of any PFCA constituent at any of the wells at the site in October 2017 (PFUnA at MW-1 with a concentration of 0.02 μg/L). This is the same well where PFOS was detected at a low concentration in October 2017. Monitoring conducted in March 2018 indicated that all PFAAs were nondetect at MW-1, including PFOS and PFUnA. The cause of these two detections in October 2017 is unknown, although it may be related to cross-contamination during sample collection in the field, or sample handling in the laboratory.

The use of radial diagrams is beneficial when evaluating spatial and temporal trends for a number of PFAS constituents across the site. If preinjection samples had been analyzed for all PFCAs instead of just PFOA, then another series could have been plotted on each radial diagram instead of the single symbol for PFOA. These radial diagrams were plotted using Visual Bio (Porewater Solutions, 2017),

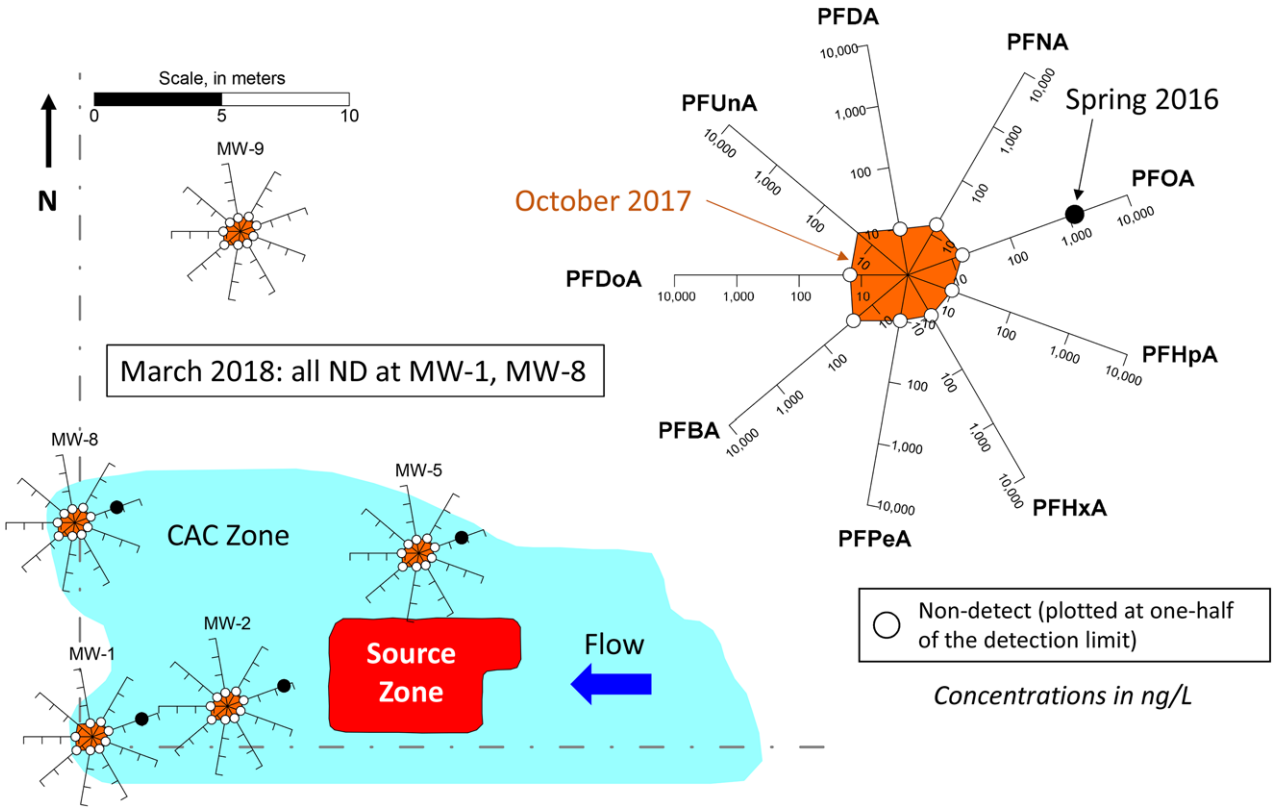

EXHIBIT 2 PFCA radial diagrams (October 2017)

which is available for free download at http://www.porewater.com/visualbio-download.html.

Exhibit 3 presents radial diagrams representing PFSAs that were analyzed in October 2017, including perfluorobutane sulfonate (PFBS), perfluorohexane sulfonate (PFHxS), PFOS, and perfluorodecane sulfonate (PFDS). Analytical results for perfluorooctane sulfonamide (PFOSA), a precursor to PFAAs, are also presented on the radial diagrams shown in Exhibit 3. Similar to Exhibit 2, nondetect symbols are shown in Exhibit 3 as well as a single symbol for PFOS preinjection concentrations (because other PFSAs were not analyzed prior to CAC injection). Exhibit 3 shows that all PFSAs were nondetect at the site except for a low concentration of PFOS detected at MW-1 as discussed above. Monitoring conducted in March 2018 indicated that all PFAAs were nondetect, which suggests that the lone detection of PFOS may be related to cross-contamination.

Exhibits 2 and 3 indicate that the postinjection PFAA concentrations are less than the method detection limits of 0.02 to 0.03 μg/L in the CAC zone, and that they have stayed low for a period of two years. These shorter term monitoring data provide valuable insights that inform on the range of isotherm properties that occurs *in situ* at the site; that is, these results may be used to rule out ranges of isotherm properties that are not realistic for the site. As shown below, these monitoring data may be used to constrain the range of PFOS-CAC isotherm properties that are applicable for evaluating remedy longevity.

Exhibit 4 shows redox radial diagrams representing trends at site wells for four redox indicators (dissolved oxygen, oxidation-reduction potential [ORP], nitrate, and sulfate), for three monitoring events: (1) Spring 2016 prior to CAC injection; (2) April 2017 (13 months after injection); and (3) October 2017 (19 months after injection). The yellow data series represent the redox indicator concentrations corresponding to the respective monitoring event. The size of the yellow data series indicates the extent to which conditions are oxidizing (i.e., aerobic) or reducing (i.e., anaerobic).

Exhibit 4a shows that prior to CAC injection, groundwater upgradient from the PFAS source zone was generally aerobic where the yellow data series are relatively large in extent (MW-4, MW-5, and MW-7). Exhibit 4a also shows that groundwater was generally anaerobic downgradient of the PFAS source zone area prior to CAC injection (MW-1, MW-2, MW-8, and MW-11). The transition from aerobic background to downgradient anaerobic conditions is probably due to the biodegradation of petroleum hydrocarbons that were generally colocated with the PFAS plume that was present prior to CAC injection. Exhibit 4b illustrates that groundwater conditions at downgradient monitoring wells (MW-1, MW-2, and MW-8) had changed from anaerobic conditions prior to the injection event, to aerobic conditions 13 months after the injection event. This change is consistent with the inclusion of oxygen-releasing material in the solution injected in spring 2016, creating sustained aerobic conditions within the injection zone.

Exhibit 4c illustrates that dissolved oxygen and ORP levels declined between April and October 2017, indicating that the oxygen-releasing material was being depleted. As shown in Exhibits 1 through 3, the presence of aerobic conditions did not cause an increase in the concentrations of PFAAs in groundwater due to potential precursor biodegradation. This may be due to low concentrations of precursors being present prior to CAC injection, or that PFAAs that may have been

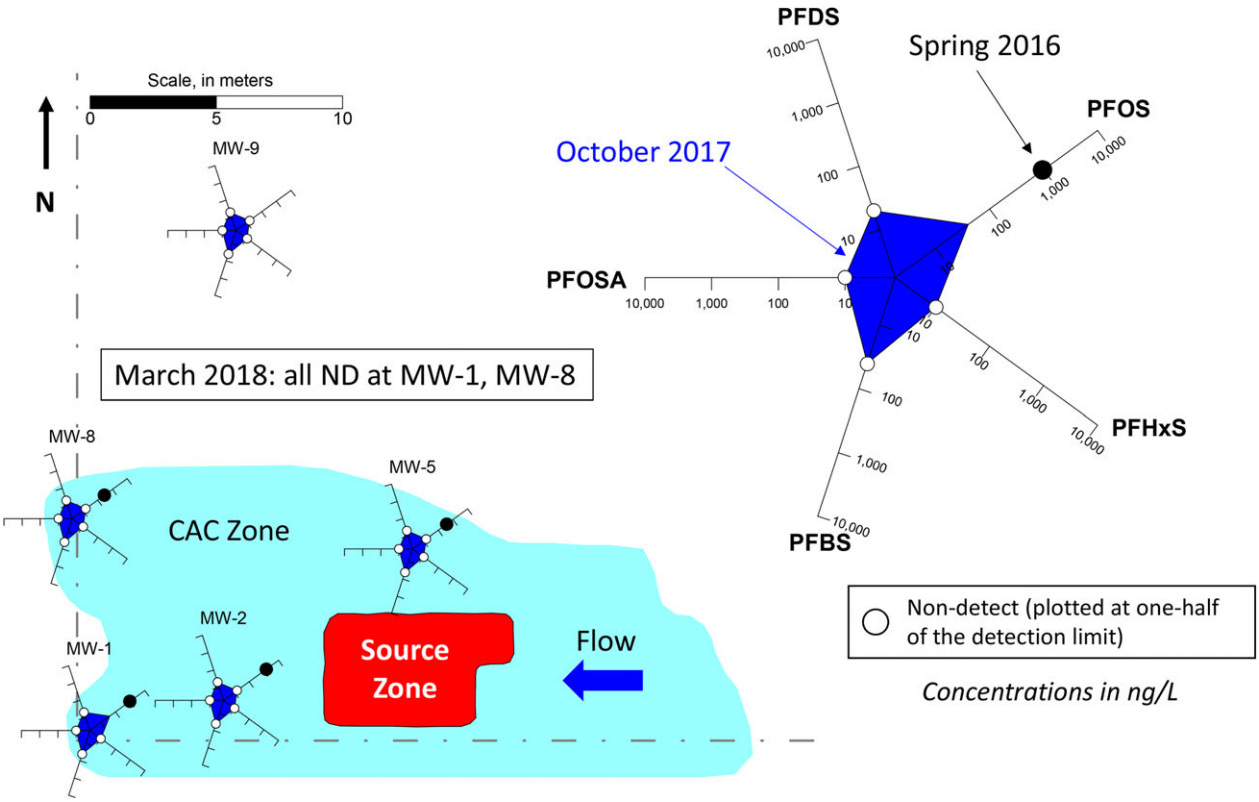

EXHIBIT 3 PFSA radial diagrams (October 2017)

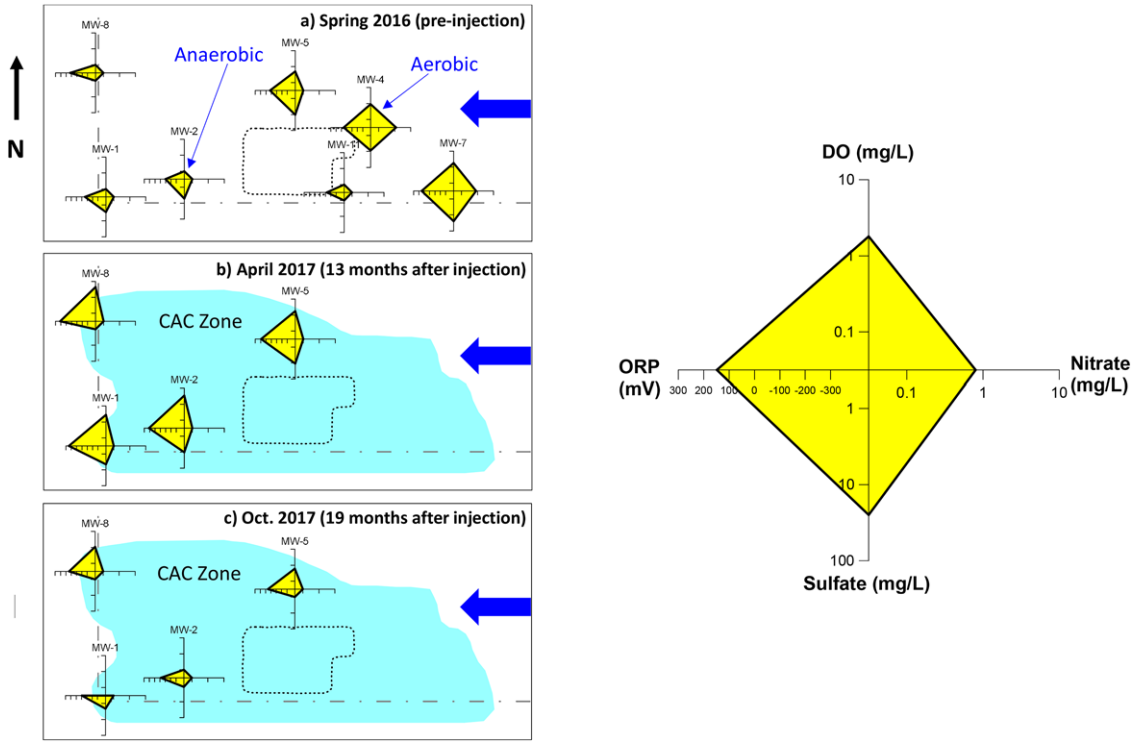

EXHIBIT 4 Redox radial diagrams (October 2017)

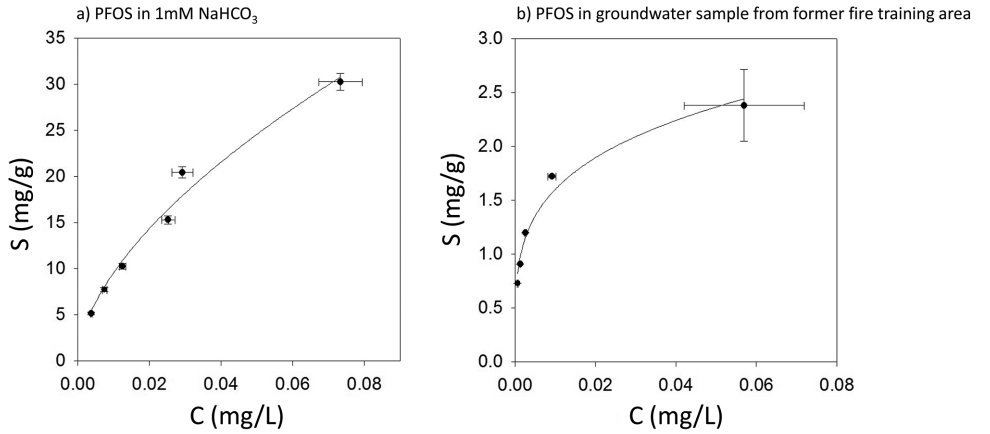

EXHIBIT 5 PFOS-CAC isotherms for a pure solution and a PFAS groundwater sample from a former fire-training area. *S* is the PFOS concentration sorbed to CAC, and *C* is the PFOS aqueous concentration

produced during aerobic biodegradation of precursors were subsequently sorbed to CAC in the soil.

3 | PFOS-CAC ISOTHERMS

PFAS sorption to *in situ*-activated carbon follows Freundlich isotherm behavior, such that the chemical concentration sorbed to CAC in soil is determined based on

$$S_{CAC} = K_f\, f_{cac}\, C^a \quad (1)$$

where S_{CAC} is the contaminant concentration sorbed to CAC in soil (milligrams per kilogram [mg/kg]); K_f is the Freundlich CAC partitioning coefficient (milligrams$^{1\text{-}a}$ liter^a per kilogram mg$^{1\text{-}a}$ L^a/kg); f_{cac} is the fraction of CAC in soil (g/g); *C* is the contaminant aqueous concentration in groundwater (milligrams per liter [mg/L]); and *a* is the Freundlich isotherm exponent (dimensionless).

K_f is sometimes referred to as the sorption capacity for a sorbent and is equal to the soil concentration that occurs in when *C* is 1 mg/L. The Freundlich isotherm exponent *a* reflects the degree of nonlinearity in the isotherm; when $a = 1$, the isotherm simplifies to the linear sorption isotherm.

When the Freundlich isotherm represents the dominant sorption mechanism, a nonlinear retardation coefficient may be estimated using

$$R_{cac} = 1 + \frac{\rho_b}{\theta}(K_f\, f_{cac}\, a\, C^{a-1}) \quad (2)$$

where R_{cac} is the retardation coefficient (dimensionless); θ is effective porosity (L/L); and ρ_b is soil dry bulk density (g/mL).

Equations (1) and (2) demonstrate that the Freundlich isotherm properties (K_f and *a*) and f_{cac} have a significant influence on the PFAS retardation coefficient associated with CAC. A previous study developed a PFOS isotherm with CAC where K_f = 55,890 mg$^{1\text{-}a}$ L^a/kg and $a = 0.47$ (Regenesis, 2016).

In this study, PFOS-CAC isotherms were determined for (1) pure solution in 1 mM $NaHCO_3$ (K_f = 142,800 mg$^{1\text{-}a}$ L^a/kg, $a = 0.59$); and (2) PFAS mixture in a groundwater sample collected in the vicinity of a former fire-training area in the United States (K_f = 4,900 mg$^{1\text{-}a}$ L^a/kg, $a = 0.24$). The groundwater sample with the PFAS mixture had a PFOS concentration of 208 μg/L, and the total detected concentrations of PFSAs, PFCAs, and (mainly fluorotelomer) precursors were 281.8, 46.9, and 60.2 μg/L, respectively. PFAS analytical results for this groundwater sample are presented in Supporting Information Table S1. PFOS, on a mass basis, was approximately 53% of the total detected PFAS in the groundwater sample. The concentration of total organic carbon (TOC) in the groundwater sample from the former fire-training area was 23.8 mg/L.

Each isotherm was determined based on batch experiments performed in triplicate. Exhibit 5 shows the charts of sorbed versus aqueous concentrations determined for these two isotherms. The isotherms were developed by adding different amounts of CAC into solution, and measuring the amount of PFOS that remained in solution (see Supporting Information for detailed information on the experimental procedure). The concentration of PFOS remaining in solution after equilibrating with CAC ranged from 4 to 70 μg/L for the 1 mM $NaHCO_3$ solution isotherm, and from 0.6 to 57 μg/L for the PFAS groundwater sample isotherm.

The difference between these two isotherms may be related to the effects of competitive sorption in the groundwater PFAS sample isotherm, due to the presence of other PFAS, TOC, and/or other co-contaminants. The groundwater sample contained 23.8 mg/L TOC. Differences in these two isotherms may also be related to differences in geochemistry between the two isotherm solutions. The effects of competitive sorption and geochemistry on PFOS-CAC isotherms are not well understood and are currently undergoing further study.

The Freundlich partitioning coefficient (K_f) is approximately 30 times lower for the groundwater sample with the PFAS mixture, relative to the isotherm determined with the PFOS single-component solution. A lower K_f associated with PFAS mixtures will tend to reduce longevity of an *in situ* CAC remedy. In contrast, the groundwater PFAS mixture isotherm has a lower Freundlich exponent (*a*), which will tend

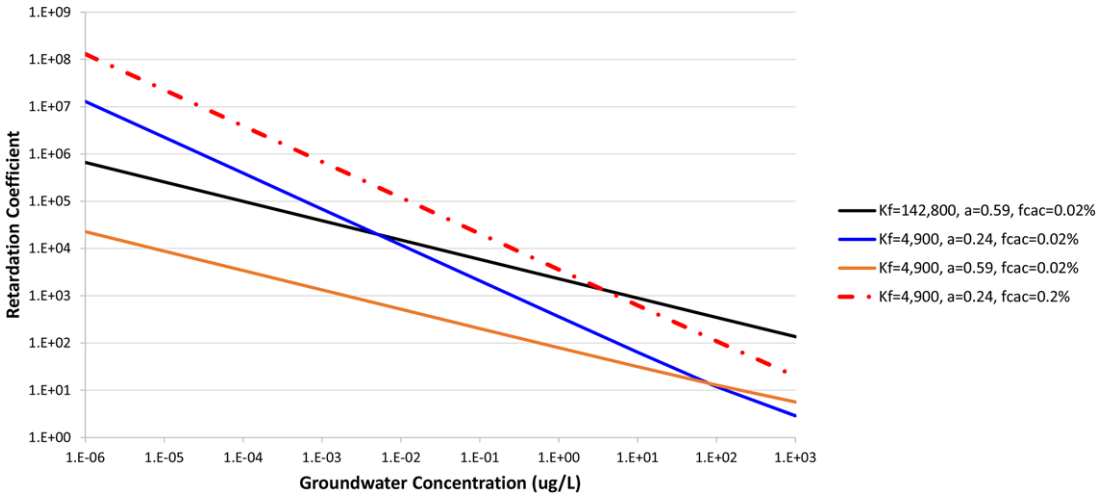

EXHIBIT 6 Retardation coefficient versus aqueous concentration of PFOS within CAC zone. K_f units are mg^{1-a} L^a/kg

to increase the longevity of an *in situ* CAC remedy when PFAS concentrations are low. PFOS-CAC isotherms are likely dependent on site-specific groundwater characteristics, and thus may need to be determined for a given site to reduce uncertainty in CAC performance.

Exhibit 6 plots the retardation coefficient (based on Equation (2)) versus the aqueous concentration of PFOS measured in groundwater after CAC injection and the subsequent mass redistribution step that is discussed further below. When modeling *in situ* CAC performance, the numerical model applies the Freundlich isotherm parameters over a larger range in aqueous concentrations than that which is utilized during the isotherm experiments. This creates uncertainty in the magnitude of the retardation factor at very low aqueous concentrations, which should be considered when evaluating model predictions.

Exhibit 6 demonstrates that, for aqueous concentrations of PFOS below approximately 0.01 μg/L, the retardation coefficient is higher for the isotherm derived from the groundwater that contained a mixture of PFAS (blue solid line) relative to the retardation coefficient associated with the solution containing only PFOS (black solid line). Even though the K_f is approximately 30 times higher for the latter solution, the Freundlich exponent *a* is more than 50% lower for the groundwater sample from the former fire-training area. This demonstrates that a small difference in the Freundlich exponent *a* can have a significant influence on the retardation coefficient.

Exhibit 6 also illustrates that a higher f_{cac} in soil will result in a proportional increase in the retardation coefficient (e.g., when f_{cac} is increased from 0.02% to 0.2%), which is also indicated by Equation (2). This indicates that the remedy performance in the long term may be engineered or improved by injecting higher concentrations of CAC.

4 | MODEL DEVELOPMENT

Prior to CAC injection, contaminant mass will be present in at least two phases (ignoring the potential for nonaqueous phase liquid): The aqueous phase (i.e., dissolved in groundwater) and sorbed to naturally occurring organic matter in soil. When CAC is injected into the subsurface, the colloidal particles will be transported through porous media and will attach to sand grains adjacent to the injection point based on typical colloidal transport behavior. After injection, contaminant mass will be redistributed into a new three-phase system: aqueous phase, sorbed to organic matter, and sorbed to the CAC. Given the high sorption capacity of activated carbon, PFAS mass will likely be redistributed predominantly in the CAC-sorbed phase.

Typical sources contributing to PFAS plumes in the subsurface include back-diffusion from lower-permeability soils such as silt and clay; rate-limited desorption from organic matter in soil; percolation to the water table from a vadose zone source; and/or dissolution from nonaqueous phase liquid (NAPL) in which the PFAS has become entrained. If CAC is injected into a PFAS source zone, it is expected (at least conservatively) that these sources will continue to persist, resulting in long-term mass loading to the CAC zone over time. Because PFAAs are not expected to undergo transformation reactions, the adsorption capacity in a CAC zone will eventually become exhausted, resulting in the eventual breakthrough of PFAAs if the long-term source continues to persist.

A numerical model may help in estimating whether and/or when a regulatory cleanup level may be exceeded in the source zone or in a downgradient plume, depending on the specifics of the CAC injection. If or when PFAS breakthrough occurs, then remedial alternatives at that future time may include reinjection of CAC into or downgradient of the original CAC zone, or utilization of another *in situ* treatment technology that may become available in the future. The main benefit of *in situ* CAC as a mass flux reduction alternative, relative to pump-and-treat (P&T), which is the most common remedial technology implemented at PFAS sites, is the passive nature of an *in situ* CAC remedy and the corresponding lower cost at some sites.

Two numerical modeling approaches were developed and applied as part of this study to simulate the longevity of CAC (i.e., time until the regulatory cleanup goal is exceeded due to PFAS breakthrough), based on the single injection event at the site:

- Incorporation of a mass redistribution step into a three-dimensional (3-D) numerical reactive transport model referred to as the *In Situ*

Remediation Model, or ISR-MT3DMS, which is described by Carey, Chapman, Parker, and McGregor (2015) and

- Development of a simplified finite-difference solution in time to evaluate the time to reach breakthrough in the center of a PFAS source zone where advective and dispersive flux is low relative to the flux of sorption onto CAC.

4.1 | Simulating mass redistribution after CAC injection

Contaminant mass in the aqueous phase prior to CAC injection is calculated using

$$M_{w,o} = C_o\ \theta\ V_s \tag{3}$$

where $M_{w,o}$ is the mass in aqueous phase prior to CAC injection (mg); C_o is the aqueous concentration prior to CAC injection (mg/L); and V_s is representative soil volume (L).

Contaminant mass sorbed to organic matter in soil is determined using

$$M_{s,o} = K_{oc}\ f_{oc}\ C_o\ \rho_b\ V_s \tag{4}$$

where $M_{s,o}$ is the mass sorbed to organic matter in soil prior to CAC injection (mg) and f_{oc} is the fraction of organic carbon (g/g).

The total contaminant mass in soil (assuming there is no NAPL present) is given by

$$M_{T,o} = C_o\ V_s(\ \theta + K_{oc}\ f_{oc}\ \rho_b\ ) \tag{5}$$

where $M_{T,o}$ is the total mass in a representative soil volume prior to CAC injection (mg).

After injection of CAC into the subsurface, the contaminant mass will be redistributed within the CAC zone. It is assumed that aqueous PFAS will adsorb rapidly to the CAC, and that equilibrium desorption of PFAS from organic matter and subsequent sorption to CAC will occur. The actual time for desorption from organic matter to occur is uncertain and will vary based on site and contaminant conditions. However, as desorption does occur into the aqueous phase, the subsequent adsorption onto CAC is expected to be rapid due to the large surface area associated with CAC. This is consistent with a previous study that observed significantly faster equilibration times for a smaller activated carbon size (i.e., PAC versus GAC), due to a larger external surface area and more functional groups being available for PFAS sorption with the smaller carbon particle size (Yu et al., 2009).

A mass-balance approach was utilized to estimate the adjusted aqueous concentration (C_{adj}) in the CAC zone after injection. To facilitate this mass balance, it was assumed that at equilibrium after redistribution, the mass sorbed to organic matter and the mass in the aqueous phase are much smaller than the mass sorbed to CAC, immediately after CAC injection. Based on the large adsorption capacity as can be seen from the PFOS isotherms (Exhibit 5), this assumption is valid for the case study discussed here, as will be demonstrated below. This assumption should be verified on a site-by-site basis.

A mass-balance approach was utilized to estimate the adjusted aqueous concentration (C_{adj}) in the CAC zone after injection.

The mass sorbed to CAC after this redistribution step (i.e., immediately after CAC injection) is calculated using

$$M_{s,CAC} = K_f\ f_{cac} C_{adj}{}^{a}\ \rho_b\ V_s \tag{6}$$

where C_{adj} is the adjusted aqueous concentration after CAC injection (mg/L).

Based on the simplifying assumption described above, and by rearranging Equations (5) and (6), the adjusted aqueous concentration after CAC injection is calculated using

$$C_{adj} = \left[\frac{C_o\ (\ \theta + \ K_{oc}\ f_{oc}\ \rho_b\ )}{K_f\ \ f_{cac}\ \rho_b}\right]^{1/a} \tag{7}$$

Using the maximum observed PFOS concentration (1.5 μg/L) at the Central Canada site as an example for C_o, the adjusted aqueous concentration after CAC injection may be calculated using Equation (6). The PFOS-CAC isotherm determined based on the PFAS mixture from a former fire-training area is used as the base case for this calculation and for the longevity modeling presented below. Based on an effective porosity (θ) of 20%, K_{oc} = 920 mg$^{1\text{-}a}$ L^a/kg (refer to Supporting Information), f_{oc} = 0.1% based on the minimum f_{oc} that represents dissolved organic carbon sorption (Delle Site, 2001), ρ_b = 1.6 g/mL, K_f = 4,900 mg$^{1\text{-}a}$ L^a/kg, a = 0.24, and f_{cac} = 0.02%, C_{adj} is calculated to be 2×10^{-9} μg/L, which corresponds to the PFOS concentration that would occur after mass is redistributed due to CAC injection.

The retardation coefficient corresponding to linear sorption to organic matter is calculated using the above parameters to be 8.4. This is orders of magnitude lower than the retardation coefficient calculated using Equation (2) for sorption of PFOS to CAC ($R_{cac} = 1 \times 10^9$), which illustrates that mass in the aqueous and organic matter-sorbed phases is negligible relative to the CAC-sorbed phase immediately after injection. The difference in retardation coefficients for organic matter and CAC adsorption supports that the simplifying assumption in the mass balance approach is reasonable for this site.

4.2 | Equilibrium mixing model

A transient EMM was developed to provide an approximate estimate of how long the CAC remedy would remain effective in the middle of a PFAS source zone (i.e., prior to breakthrough above regulated concentration limits). The EMM is based on a mass balance implemented using a finite-difference solution in time. The EMM is also based on the assumption that there is ongoing PFAS mass discharge into groundwater in the source zone after CAC injection, due to contributions from

back-diffusion, rate-limited desorption, infiltration to the water table from a source in the vadose zone, and/or NAPL dissolution. The mass discharge term in the EMM may also represent the plume strength directly upgradient of a reactive barrier where CAC is injected to intercept a plume.

The EMM simulates the aqueous concentration over time in a single mixing cell in the middle of a source zone. The net fluxes into and out of the grid cell due to advection and dispersion are assumed to be equal, resulting in accumulation in the cell due to mass discharge from the source. The EMM is applicable when the rate of sorptive flux onto the CAC is significantly larger than the net advective and dispersive out of the mixing cell. The EMM simulates the aqueous concentration over time in the mixing cell, accounting for sorption to CAC. Results of this model may be used to estimate the earliest time at which breakthrough may occur due to long-term loading of PFAS mass within the CAC zone. The benefit of this finite-difference solution is that it can be implemented within a spreadsheet, so a more sophisticated numerical model is not required to develop a preliminary estimate of CAC longevity in the source zone. The limitation of this approach is that it will underestimate the longevity in areas where the net advective and dispersive fluxes out of the grid cell are relatively significant.

The EMM is applicable when the rate of sorptive flux onto the CAC is significantly larger than the net advective and dispersive out of the mixing cell.

The initial aqueous concentration in the model at a time of 0 (C_{adj}) is calculated based on Equation (7). At time step t, the change in aqueous concentration, and the retardation coefficient in the grid cell, are calculated using

$$R^t = 1 + \frac{\rho_b}{\theta} K_f f_{cac} a (C^{t-1})^{a-1} \quad (8)$$

$$\Delta C^t = \left(Md^t_{src} \Delta t\right) / \left(V_{cell} R^t \theta\right) \quad (9)$$

$$C^t = C^{t-1} + \Delta C^t \quad (10)$$

where R^t is the retardation coefficient at the current time step; C^{t-1} is the aqueous concentration at the previous time step (mg/L); ΔC^t is change in aqueous concentration at the current time step (mg/L); C^t is aqueous concentration at the current time step (mg/L); $Md_{src}{}^t$ is source mass discharge into the grid cell at the current time step (mg/d); Δt is time step duration (d); and V_{cell} is the volume of the cell (L).

The EMM includes functionality for representing an exponential decline over time in the source zone mass discharge (Md_{src}), to represent sources that deplete over time. For example, examination of results from an analytical solution for back-diffusion indicated that a back-diffusion source decline half-life of 20 to 30 years is reasonable for some sites (refer to Supporting Information).

Because the EMM does not represent flux leaving the cell by advection or dispersion, the simulated aqueous concentrations will eventually exceed the initial aqueous concentration. A check is included in the EMM to detect when the simulated aqueous concentration reaches the maximum observed concentration prior to CAC injection. It is also possible to represent an exponential decline in this maximum initial concentration in the EMM based on the source decline discussed above, using the same half-life as the source zone mass discharge (Md_{src}).

As shown below, for the cases examined here, the results from the EMM model are similar to the results from ISR-MT3DMS, which accounts for PFAS transport by advection and dispersion in the source zone.

5 | *IN SITU* CAC LONGEVITY ASSESSMENT

The models described above (ISR-MT3DMS and the EMM) were used to predict the longevity of *in situ* CAC effectiveness at the Central Canada site in the middle of the source area and at the downgradient extent of the CAC zone, which is approximately 10 m downgradient of the source area. Longevity is defined in this study to represent the time between CAC injection and when the PFOS concentration exceeds the regulatory cleanup level. For this study, the regulatory cleanup level was assumed to be the Health Canada drinking water screening value for PFOS of 0.6 μg/L.

5.1 | Flow and transport model construction

A 2-D areal model domain was constructed to represent groundwater flow and solute transport at the site. MODFLOW (McDonald & Harbaugh, 1988) was used to simulate steady-state groundwater flow based on the average site characteristics for hydraulic conductivity (2.6 m/d). The model grid was based on a consistent 2 m spacing outside of the CAC zone, and 0.5 m within the CAC zone with a transition spacing of 1 m between these two areas. A uniform saturated thickness of 0.8 m was assumed, consistent with the thickness of the PFAS plume at the site (McGregor, 2018). Constant head boundary conditions were used to replicate the observed average horizontal hydraulic gradient of 0.06 m/m. Because the area was industrial and mostly covered at the ground surface, it was assumed that the rate of infiltration was zero except for a small rate used in the source area of 0.1 inch/year, which was used to simulate a PFAS mass discharge in the source area when coupled with the reactive transport model.

The ISR-MT3DMS reactive transport model was first used to simulate the development of a relatively steady PFOS plume just prior to CAC injection, modeled to occur at a simulation time of 1,500 days. The transport model utilized a time step of 1 day. The longitudinal and transverse horizontal dispersivities were simulated to be 1 m and

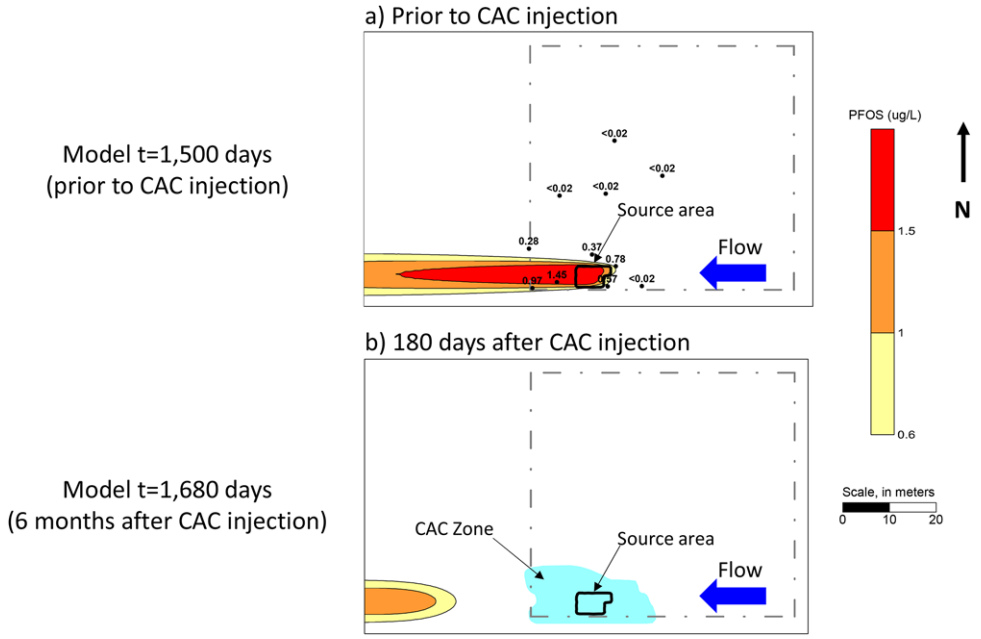

EXHIBIT 7 Simulated plume detachment after CAC injection for baseline case. The minimum PFOS concentration contour of 0.6 μg/L is based on the drinking water screening value adopted by Health Canada (July 2018). PFOS in the CAC zone is simulated to be below analytical detection limits

0.1 m, respectively. The source area mass discharge was calibrated to provide a general match to the PFOS plume observed at the site. Exhibit 7a shows the simulated PFOS plume based on a calibrated source area mass discharge rate of approximately 0.6 gram per year over a source area of 30 m^2. Observed preinjection PFOS monitoring well concentrations are also shown in Exhibit 7a, demonstrating that there is a reasonable match between the simulated and observed plumes prior to CAC injection.

A mass discharge decline half-life of 30 years was specified to represent a gradual decline in mass discharge over time. (ISR-MT3DMS provides the option to simulate an exponential decline rate for recharge sources.) The ISR-MT3DMS model incorporating Equation (7) was used to calculate the postinjection aqueous PFOS concentration, immediately after the redistribution of mass. In the ISR-MT3DMS model, the linear sorption isotherm was used to represent sorption to organic matter outside the CAC zone at all times, and within the CAC zone prior to the simulated injection time of 1,500 days. The Freundlich isotherm was used to simulate PFOS sorption to CAC in the mass flux reduction zone after the simulation time of 1,500 days.

The extent of the CAC zone was defined as an input to the model based on the locations of the temporary injection wells. As discussed above, the radius of influence for CAC was conservatively assumed to be 3 m around each injection point, which is less than the distribution of CAC during postinjection monitoring. The PFOS-CAC isotherm for the PFAS mixture from the former fire-training area was utilized for the base-case simulations (K_f = 4,900 mg^{1-a} L^a/kg and a = 0.24). There is uncertainty in the site-specific PFOS-CAC isotherm that is representative of the Central Canada site, relative to the isotherm determined for the former fire-training area. These model simulations are conducted to illustrate the sensitivity of CAC longevity to various parameters, and to evaluate if the range in possible Freundlich isotherm properties may be narrowed by comparing model simulations to observed conditions post-CAC injection.

For the base-case model simulation, an f_{cac} of 0.02% was used, based on the average f_{cac} measured at the site (McGregor, 2018). Other transport model parameters are consistent with those described above for the example PFOS C_{adj} calculation. The total simulation period extended to 100 years after CAC injection, for a total simulation time of 38,000 days.

Exhibit 7b presents the simulated PFOS plume at a time of 180 days after CAC injection (i.e., total simulation time of about 1,680 days). The minimum concentration contour (0.6 μg/L) represents the Health Canada PFOS screening value. Simulated concentrations in the CAC zone were orders of magnitude below the PFOS detection limit, due to the high CAC adsorption capacity for PFOS. The model simulation is consistent with groundwater sampling conducted at monitoring wells within the CAC 6 months after CAC injection, where PFOS was not detected at any wells with a detection limit of 0.03 μg/L. Exhibit 7b also demonstrates the simulated detachment of the PFOS plume downgradient of the CAC zone, which was caused by the effective sorption of PFOS within the CAC zone.

Exhibit 8a shows the preinjection PFOS mass distribution on the site, which illustrates that most of the PFOS mass was sorbed to organic matter, and only a small proportion of PFOS mass was in the aqueous phase. This is consistent with the preinjection retardation coefficient of 8.4 for PFOS. Exhibit 8b shows the total PFOS mass distribution within the CAC zone, after equilibration with CAC according to Equation (7). Exhibit 8b demonstrates that PFOS mass is almost entirely sorbed to CAC. Within the CAC zone and prior to CAC injection, the model simulated a total PFOS mass of 30.4 mg in the aqueous phase and 223.5 mg sorbed to native organic matter, for a total mass of 253.9 mg. Immediately after CAC injection, ISR-MT3DMS simulated

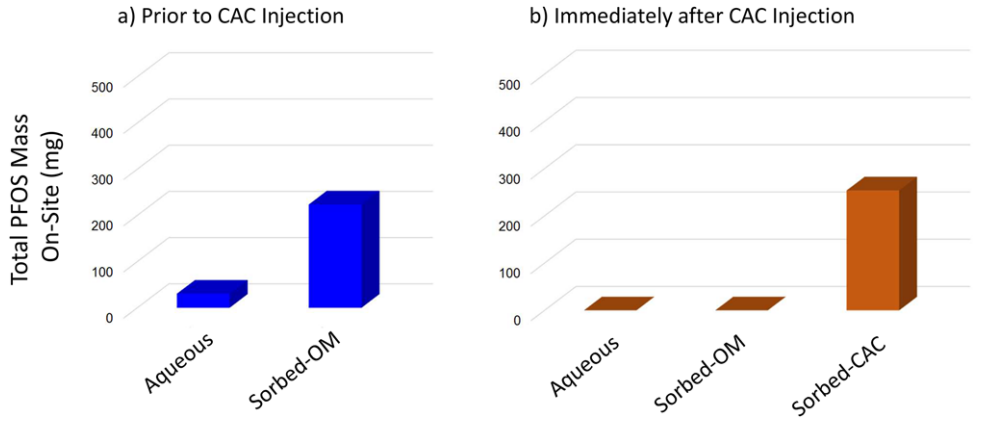

EXHIBIT 8 PFOS mass-balance pre- and post-CAC injection. Sorbed-OM refers to PFOS sorbed to native organic matter

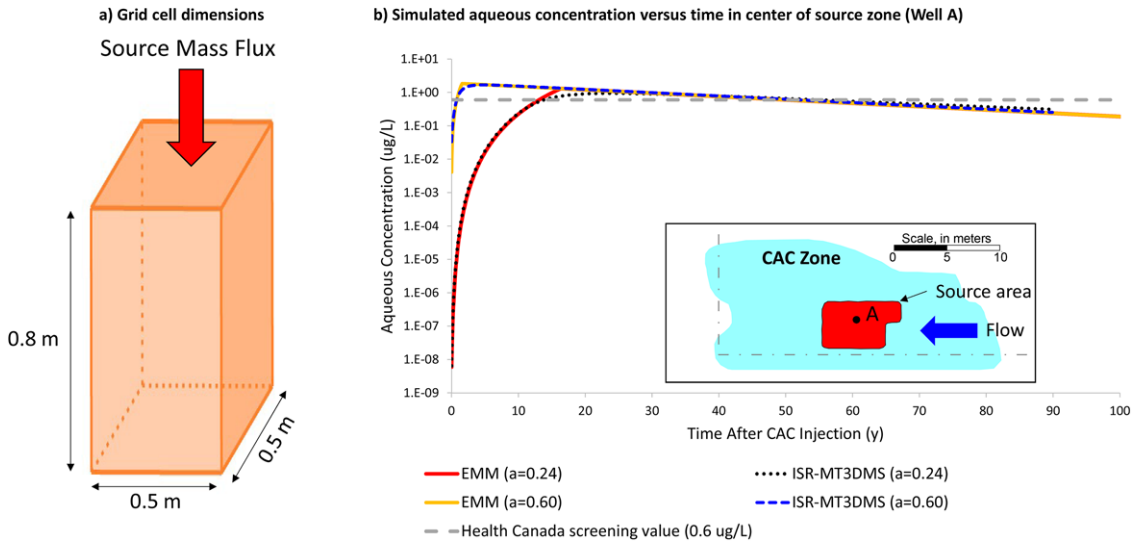

EXHIBIT 9 Comparison of EMM and ISR-MT3DMS simulated concentrations versus time in the center of the source area. ISR-MT3DMS simulated concentrations are at observation well A shown on the inset map. f_{cac} for simulations was 0.02%

the total PFOS mass in this same area to be 1.0×10^{-7} mg in the aqueous phase, and 7.4×10^{-7} mg sorbed to native organic matter. PFOS mass sorbed to CAC was simulated to be approximately 253.9 mg. This distribution confirms the mass balance assumption that the mass in the aqueous and native organic matter-sorbed phases is negligible relative to the mass sorbed to CAC.

5.2 | CAC longevity modeling

5.2.1 | Breakthrough time at center of source area (EMM versus ISR-MT3DMS)

The EMM solution (i.e., Equations (8)–(10)) results were compared with ISR-MT3DMS simulations that include advective and dispersive fluxes across the source area.

Exhibit 9a shows the dimensions of the single grid cell modeled using the EMM, where only the source discharge is considered as a cumulative flux into the grid cell. The length and width of the EMM grid cell are consistent with the grid resolution in ISR-MT3DMS (i.e., 0.5 m × 0.5 m, and the saturated thickness of the grid cell is 0.8 m). Two different scenarios were used for comparison of the EMM and ISR-MT3DMS under a range of longevity conditions in the source area: one with Freundlich exponent $a = 0.24$ (base case) and one with $a = 0.6$ (representing the exponent determined for a pure PFOS solution isotherm). Both scenarios used $K_f = 4{,}900$ mg^{1-a} L^a/kg, $f_{cac} = 0.02\%$, and a source mass discharge decline half-life of 30 years.

Exhibit 9b compares the EMM and ISR-MT3DMS simulated concentrations in the center of the source zone for these two scenarios. The location of the observation well specified in ISR-MT3DMS (well A) is shown in the inset map in Exhibit 9b. Exhibit 9b demonstrates that the simulated PFOS concentrations over time in the EMM were similar to the results from ISR-MT3DMS, which indicates that the EMM assumption of negligible advective and dispersive fluxes relative to the CAC sorption flux is reasonable for the center of the source area at this site.

The base-case scenario ($a = 0.24$) resulted in a breakthrough time of approximately 14 years, corresponding to the time after CAC injection when the simulated PFOS concentration exceeded the Health Canada screening value of 0.6 μg/L. However, as shown below, the breakthrough time at the downgradient extent of the CAC zone (10 m downgradient of the source area) is much longer than the breakthrough time

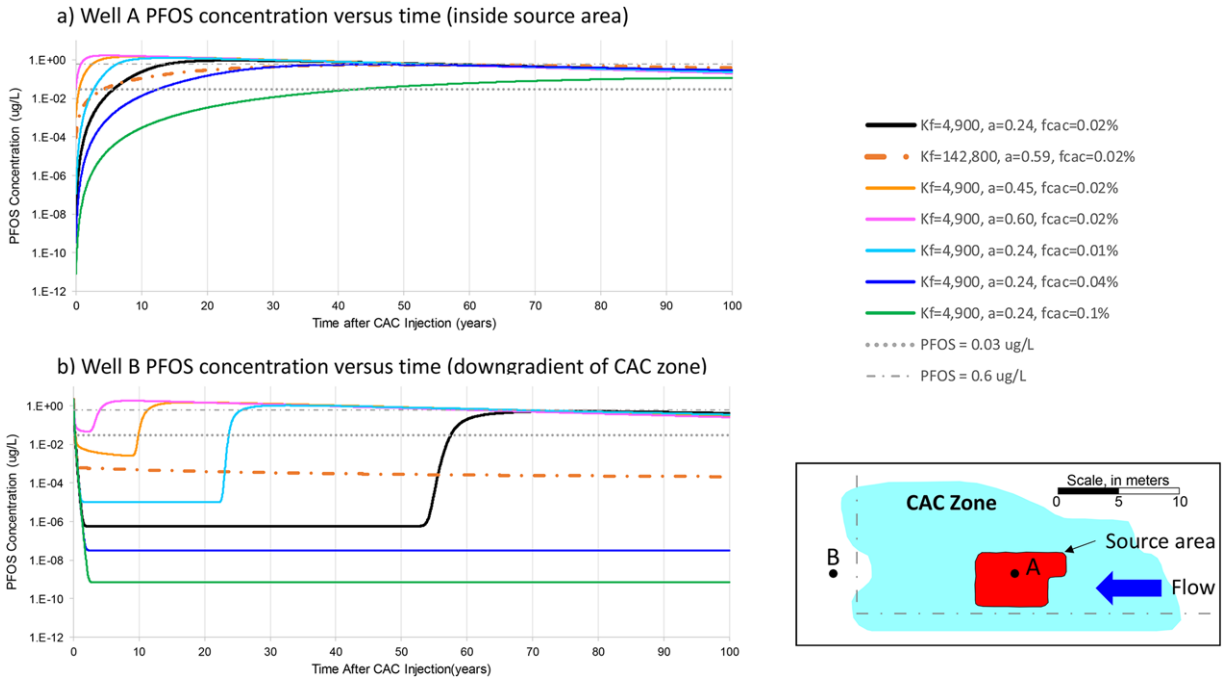

EXHIBIT 10 Breakthrough timeframe sensitivity analysis. $t = 0$ corresponds to when CAC injection was simulated. K_f units are mg^{1-a} L^a/kg

in the source area. Therefore, the EMM has limited applicability when a CAC buffer zone is incorporated downgradient of the source area and may significantly underestimate the longevity in this case. As a comparison, the breakthrough time corresponding to a greater Freundlich exponent of $a = 0.6$ is only 0.8 year, indicating that this exponent has a significant influence on the sorption of PFOS and the longevity of a CAC remedy.

5.2.2 | Breakthrough time at downgradient boundary of the CAC zone (ISR-MT3DMS)

Exhibits 10a and 10b present simulated PFOS concentrations versus time at two observation wells in the model domain: well A in the source zone and well B directly downgradient of the CAC zone. The base-case simulation utilized the PFOS isotherm determined with the PFAS groundwater mixture ($K_f = 4{,}900$ mg^{1-a} L^a/kg and $a = 0.24$) and $f_{cac} = 0.02\%$. Three additional isotherm scenarios were simulated to evaluate the sensitivity of the breakthrough curves to isotherm parameters (all using $f_{cac} = 0.02\%$): (1) $K_f = 142{,}800$ mg^{1-a} L^a/kg and $a = 0.59$ (PFOS pure solution isotherm); (2) $K_f = 4{,}900$ mg^{1-a} L^a/kg and $a = 0.45$; and (3) $K_f = 4{,}900$ mg^{1-a} L^a/kg and $a = 0.60$. Three additional scenarios were simulated using the base-case isotherm and f_{cac} values of 0.01%, 0.04%, and 0.1%.

Exhibit 10a shows that PFOS concentrations in the source zone increase above the detection limit of 0.03 μg/L at a time of 5.7 years after CAC injection, and increases above the Health Canada screening value of 0.6 μg/L after 14 years. In comparison, the scenario using $K_f = 4{,}900$ mg^{1-a} L^a/kg and $a = 0.45$ resulted in a detectable PFOS concentration in the source zone at a time of 0.5 years after CAC injection, and the scenario using $a = 0.60$ always had detectable PFOS in the source zone. These two isotherm scenarios do not match site conditions where PFOS was not detected in any site monitoring wells over the two-year period since CAC injection, with the exception of one low detection that may have been due to cross-contamination. Therefore, these two isotherms are not representative of the sorption characteristics of CAC in the geochemical conditions at this site.

Exhibit 10b illustrates the PFOS concentration versus time curves for well B, which is 3.2 m downgradient of the CAC zone and 11.7 m downgradient of the source area. Comparison of the curves in Exhibits 10a and 10b shows that breakthrough occurs much later at well B than at well A (in the source area). For example, PFOS exceeds the detection limit at well A in the source area at a time of 5.7 years after CAC injection, but only exceeds the detection limit at well B after 62 years. This delay in the downgradient breakthrough is due to the 10 m long CAC buffer zone downgradient of the source area. This demonstrates the benefit that may be derived by extending the length of the CAC buffer zone (parallel to groundwater flow) on the longevity of an *in situ* CAC remedy, or by increasing the retention time in a permeable CAC barrier wall being used to intercept a PFAS plume. The model can be used to investigate various schemes for CAC-based remediation and for conducting cost–benefit analyses.

The base-case scenario in Exhibit 10b shows that the PFOS concentration does not exceed the Health Canada screening value of 0.6 μg/L, even though concentrations did eventually rise at well B, because the source mass discharge was simulated to have a decline half-life of 30 years. This base-case simulation predicts that the *in situ* CAC remedy will be successful at mitigating future plume migration downgradient of the site. There is uncertainty regarding this outcome, related to uncertainty in the *in situ* PFOS-CAC isotherm, mass discharge decline half-life, and even in future regulatory cleanup levels, which may be significantly lower than 0.6 μg/L. However, given the relatively low cost to implement the CAC remedy at this site, and the ability to adapt the

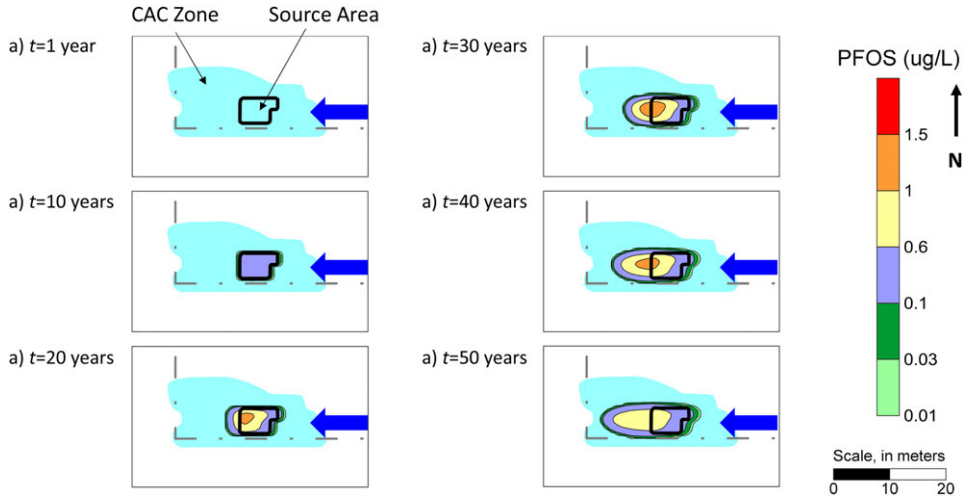

EXHIBIT 11 PFOS concentration contours over time. $K_f = 4{,}900\ mg^{1-a}\ L^a/kg$, $a = 0.24$, and $f_{cac} = 0.02\%$. Light blue shading represents the CAC zone and the thick black outline represents the source area. The dashed line represents the site boundary. Times correspond to the time after CAC injection. See Exhibit 1 for site monitoring well locations

remedy in the future by reinjecting into the existing CAC zone or to extend the length of the CAC buffer zone, this remedy may be viable at other PFAS sites. The only other alternative presently available at PFAS sites is P&T that would have to be operated for decades due to the ongoing nature of the PFAS source. It is also possible to combine P&T in a remedy, such as using P&T at a site boundary where PFAS concentrations are higher, and implementing CAC barriers downgradient to mitigate plume migration.

Exhibit 10b also demonstrates the influence that f_{cac} has on the remedy longevity. PFOS exceeds the detection limit at well B at a time of 24 years after CAC injection when the average f_{cac} is 0.01%, which is approximately 60% sooner than the scenario using $f_{cac} = 0.02\%$. Breakthrough did not occur at well B during the 100-year simulation for $f_{cac} = 0.04\%$ and 0.1%. This demonstrates that the longevity of the *in situ* CAC remedy may be engineered by increasing f_{cac} and the corresponding CAC concentration in the injected solution. Alternatively, the length of the CAC zone can be extended in the future based on long-term monitoring results to transfer a portion of the remedy cost into the future.

Exhibit 11 presents simulated PFOS concentration contours for the base-case scenario at simulation times of 1, 10, 20, 30, 40, and 50 years after CAC injection. The minimum PFOS concentration contour is 0.03 μg/L, which represents the PFOS detection limit. At t = 1 year after CAC injection, simulated PFOS concentrations are below the detection limit throughout the CAC zone, which is consistent with observed conditions. At a time of 10 years, PFOS is predicted to be detectable within the source area but still below the Health Canada screening value of 0.6 μg/L. At this time, PFOS is predicted to remain below the detection limit outside of the source area.

As concentrations continue to increase in the source area with time, the concentrations downgradient of the source area begin to increase above 0.6 μg/L. Expansion of the plume beyond the source area is slow due to retardation from sorption to CAC in the downgradient buffer zone. Two observation points were used in the model to estimate the rate of retardation of the front of the plume, which is defined for this assessment as the contour representing the PFOS detection limit of 0.03 μg/L. Both observation points are on a flow path within the CAC zone; one observation point is situated 2 m downgradient of the source area, and the second observation point is situated 5 m downgradient of the first point. The front of the plume reached the first point on the flow path at a time of 18.4 years after CAC injection, and the plume front reached the second point at a time of 40.4 years. This corresponds to an average retardation coefficient of 1,250 for the plume front within the CAC zone, downgradient of the source area.

Installing monitoring wells in the CAC buffer zone would allow detection of PFAS migration. Given the slow transport through the CAC buffer zone, there would be sufficient time to implement additional measures to slow plume movement, such as injection of additional CAC or other alternatives.

6 | CONCLUSIONS AND RECOMMENDATIONS

Various visualization and modeling methods were used to evaluate the performance of *in situ* CAC at a PFAS site in Central Canada. Redox radial diagrams demonstrate that redox conditions within and downgradient of the source area were aerobic as a result of the oxygen-releasing materials included with the injected solution. Monitoring data indicate that this did not influence the effectiveness of the CAC remedy with respect to PFAS immobilization.

Laboratory isotherms were derived for two solutions mixed with CAC: (1) PFOS in 1 mM $NaHCO_3$ and (2) a groundwater sample with PFOS among other PFAS from a former fire-training area in the United States. The isotherm parameters for the pure PFOS solution were $K_f = 142{,}800\ mg^{1-a}\ L^a/kg$ and $a = 0.59$, and the isotherm for the PFAS groundwater sample had $K_f = 4{,}900\ mg^{1-a}\ L^a/kg$ and $a = 0.24$. The difference between these two isotherms is likely related to the effects of competitive sorption due to the presence of other PFAS, native organic matter, and/or other co-contaminants in the groundwater

sample. Isotherm differences may also be related to geochemical differences between the two solutions used. The effects of competitive sorption and geochemistry on CAC isotherms require further study. It is recommended that site-specific PFAS-CAC isotherms be determined to reduce uncertainty in longevity predictions.

A mass-balance approach was developed to facilitate the numerical modeling of mass redistribution after CAC injection, when mass transitions from a two-phase system (aqueous and sorbed to organic matter) to a three-phase system, which also includes mass sorbed to CAC. A simplifying assumption in this mass balance is verified to be applicable at this site, whereby the redistributed mass after CAC injection is predominantly in the CAC-sorbed phase.

An EMM was developed to simulate aqueous concentrations over time in a single grid cell in the center of a PFAS source area after CAC injection, based on a mass balance. The EMM is demonstrated, based on comparison with ISR-MT3DMS, to be applicable in areas where advective and dispersive fluxes are low relative to the CAC sorptive flux.

The redistribution mass-balance approach was incorporated into a 3-D reactive transport model (ISR-MT3DMS), to facilitate an assessment of the longevity of *in situ* CAC within and downgradient of a source area. ISR-MT3DMS simulations indicate that the remedy will be effective in the long-term at the site with respect to PFOS, in part because of the relatively high Health Canada screening value for PFOS of 0.6 μg/L.

As with any long-term model prediction, there is uncertainty with these results, primarily with respect to the *in situ* isotherm parameters (K_f and a). A sensitivity analysis was used to demonstrate that several possible isotherms were not realistic because the model simulations were inconsistent with observed conditions. Model results also showed that the plume front is highly retarded within the CAC zone. Implementation of a CAC buffer zone downgradient of a contaminant source area provides an important opportunity for conducting long-term monitoring to confirm when additional CAC injection is required. The model was also used to demonstrate that *in situ* CAC longevity may be engineered by adjusting the CAC concentration in the injected solution, assuming that f_{cac} is proportional to the injected solution concentration.

Given the relatively low cost to implement the CAC remedy at this site, and the ability to adapt the remedy in the future by reinjecting into the existing CAC zone or to extend the length of the CAC buffer zone, this remedy may be viable at other PFAS sites. The only other alternative presently available at PFAS sites is P&T that would have to be operated for decades due to the ongoing nature of the PFAS source. It is also possible to combine P&T and CAC in a site management strategy, such as using P&T at a site boundary where PFAS concentrations are higher, and implementing CAC barriers downgradient to mitigate plume migration.

ACKNOWLEDGMENTS

The authors would like to thank Dr. Kristen Thoreson and Dr. Jeremy Birnstingl at Regenesis for their insightful comments during this study. We would also like to thank Dr. Charles Schaefer at CDM Smith for providing the PFAS groundwater sample.

REFERENCES

Appleman, T. D., Higgins, C. P., Quinones, O., Vanderford, B. J., Kolstad, C., Zeigler-Holady, J. C., & Dickenson, E. R. V. (2014). Treatment of poly- and perfluoroalkyl substances in U.S. full-scale water treatment systems. *Water Research*, *51*, 246–255.

Avendano, S. M., & Liu, J. (2016). Production of PFOS from aerobic soil biotransformation of two perfluoroalkyl sulfonamide derivatives. *Chemosphere*, *119*, 1084–1090.

Carey, G. R., Chapman, S. W., Parker, B. L., & McGregor, R. (2015). Application of an adapted version of MT3DMS for modeling back-diffusion remediation timeframes. *Remediation Journal*, *25*(4), 55–79.

Carey, G. R., Van Geel, P.J., Wiedemeier, T. H., & McBean, E. A. (2003). A modified radial diagram approach for evaluating natural attenuation trends for chlorinated solvents and inorganic redox indicators. *Ground Water Monitoring & Remediation*, *23*(4), 75–84.

Carey, G. R., Wiedemeier, T. H., Van Geel, P. J., McBean, E. A., Murphy, J. R., & Rovers, F. A. (1999). SEQUENCE visualization of natural attenuation trends at Hill Air Force Base, Utah. *Bioremediation Journal*, *3*(4), 379–393.

Delle Site, A. (2001). Factors affecting sorption of organic compounds in natural sorbent/water systems and sorption coefficients for selected pollutants: A review. *Journal of Physical and Chemical Data Review*, *30*(1), 187–439.

Harding-Marjanovic, K. C., Houtz, E. F., Yi, S., Field, J. A., Sedlak, D. L., & Alvarez-Cohen, L. (2015). Aerobic biotransformation of fluorotelomer thioether amido sulfonate (Lodyne) in AFFF-amended microcosms. *Environmental Science & Technology*, *49*(13), 7666–7674.

Hatton, J., Holton, C., & DiGuiseppi, B. (2018). Occurrence and behavior of per- and polyfluoroalkyl substances from aqueous film-forming foam in groundwater systems. *Remediation Journal*, *28*(2), 89–99.

Health Canada. (2018). Drinking water screening values: Perfluoroalkylated substances. *Water Talk*. Retrieved from https://www.canada.ca/en/services/health/publications/healthy-living/water-talk-drinking-water-screening-values-perfluoroalkylated-substances.html

McCleaf, P., Englund, S., Ostlund, A., Lindegren, K., Wiberg, K., & Ahrens, L. (2017). Removal efficiency of multiple poly- and perfluoroalkyl substances (PFASS) in drinking water using granular activated carbon (GAC) and anion exchange (AE) column tests. *Water Research*, *120*, 77–87.

McDonald, M. G., & Harbaugh, A. W. (1988). *A modular three-dimensional finite difference ground-water flow model* (586 pp.). Reston, VA: U.S. Geologic Survey. https://doi.org/10.3133/twri06A1

McGregor, R. (2018). In situ treatment of PFAS-impacted groundwater using colloidal activated carbon. *Remediation Journal*, *28*, 33–41.

Porewater Solutions. (2017). *Visual Bio™ radial ciagrams for visualizing natural and enhanced chemical degradation trends: V1.1 user's guide*. Ottawa, Ontario: Porewater Solutions.

Regenesis. (2016). *PlumeStop® technical bulletin 5.1: In situ containment of PFOA and PFOS using PlumeStop® Liquid Activated Carbon™*. San Clemente, CA: Author.

U.S. Environmental Protection Agency (USEPA). (2018, April). *Remedial technology fact sheet – Activated carbon-based technology for in situ remediation, EPA 542-F-18-001*. Washington, DC: Author.

U.S. Environmental Protection Agency (USEPA). (2016a). Drinking water health advisory for perfluorooctane sulfonate (PFOS). Retrieved from https://www.epa.gov/sites/production/files/2016-05/documents/pfos_health_advisory_final_508.pdf

U.S. Environmental Protection Agency (USEPA). (2016b). Drinking water health advisory for perfluorooctanoic acid (PFOA). Retrieved from https://www.epa.gov/sites/production/files/2016-05/documents/pfoa_health_advisory_final-plain.pdf

Yu, Q., Zhang, R., Deng, S., Huang, J., & Yu, G. (2009). Sorption of perfluorooctane sulfonate and perfluorooctanoate on activated carbons and resin: Kinetic and isotherm study. *Water Research*, *43*, 1150–1158.

AUTHORS' BIOGRAPHIES

Grant R. Carey, PhD, P Eng, is President of Porewater Solutions in Ottawa, Ontario. Dr. Carey specializes in groundwater modeling, NAPL characterization and remediation, contaminant transport, back-diffusion, and environmental forensics. Dr. Carey also founded the PFAS Remediation Research Group. He received a BASc from the University of Waterloo, an M Eng from Carleton University, and a PhD from the University of Guelph.

Rick McGregor, MSc, MBA, is a hydrogeologist with In Situ Remediation Services Ltd based in Canada. McGregor has a BSc in geology and MSc in hydrogeology and geochemistry from the University of Waterloo along with an MBA from Wilfrid Laurier University. Rick has over 27 years of experience in research, consulting, and contracting. His current focus is on the remediation of impacted groundwater.

Anh Le-Tuan Pham, PhD, is an Assistant Professor of Civil and Environmental Engineering at the University of Waterloo. His research group investigates contaminant fate and transformation. The current research focuses on developing novel technologies for the remediation of contaminated soil and groundwater, treatment of oil sands process water, and removal of emerging contaminants. He received his BS in Chemical Engineering from the Hanoi University of Technology, and MS and PhD in Civil and Environmental Engineering from the University of California, Berkeley.

Brent Sleep, PhD, P Eng, conducts hybrid research with laboratory experimentation, field studies, and computer modeling to determine the fate and transport of organic chemicals in the subsurface and surface aquatic environments. More specifically, Dr. Sleep's research is dedicated to developing innovative methods for remediation of soil and groundwater contamination, with a focus on organic contaminants. His research group is working on a variety of *in situ* subsurface remediation methods, conducting laboratory and computer modeling studies of bioremediation, thermal remediation, and the applications of chemical oxidants and nanoscale zero valent iron for subsurface remediation. His group is also investigating the transport of pathogens in fractured rock aquifers. Dr. Sleep received a BASc, MASc, and PhD from the University of Waterloo.

Seyfollah Gilak Hakimabadi, MS, is a PhD student in the Department of Civil and Environmental Engineering at the University of Waterloo. He received a BS in Chemical Engineering from the Amirkabir University of Technology, and an MS in Chemical Engineering from the Ferdowsi University of Mashhad.

SUPPORTING INFORMATION

Additional supporting information may be found online in the Supporting Information section at the end of the article.

How to cite this article: Carey GR, McGregor R, Pham AL-T, Sleep B, Hakimabadi SG. Evaluating the longevity of a PFAS *in situ* colloidal activated carbon remedy. *Remediation*. 2019;29:17–31. https://doi.org/10.1002/rem.21593